Distributed Compression and Transmission with Energy Harvesting Sensors

Rajeev Gangula*, Deniz Gündüz§, and David Gesbert*
*Mobile Communications Department, Eurecom, France
§Dept. of Electrical and Electronic Engineering, Imperial College London, UK
Email: {gangula,gesbert}@eurecom.fr, d.gunduz@imperial.ac.uk

***Abstract*—We determine the achievable distortion region when the correlated source samples are transmitted by two energy harvesting (EH) sensor nodes to the destination over orthogonal fading channels. A time slotted system is considered in which the energy and the source samples arrive at the beginning of each time slot (TS), and both the correlation between source samples at the two nodes and fading coefficients change over time but remain constant in each TS. Assuming non-causal knowledge of these time-varying source statistics, energy arrivals and the channel gains, i.e., under the offline optimization framework, we obtain the optimal transmission and coding schemes that achieve the points on the Pareto boundary of the total distortion region. An iterative directional 2D waterfilling algorithm is proposed to obtain two specific points on this boundary.**

I. Introduction

A wireless sensor node collects samples of a physical phenomenon in its surrounding environment, processes, and communicates these samples to a fusion center over a wireless radio channel. A network of such nodes can be used to gather information about a time varying process that is possibly correlated across space and time. The main bottleneck in traditional or battery run sensor networks is the limited available energy, which constraints the lifetime of the sensor network. EH technology offers an attractive solution to the network lifetime problem [1]. EH nodes can scavenge energy from the environment (typical sources are solar, wind, vibration, thermal, etc.) [2], therefore, in principle, one can guarantee infinite lifetime without the need of replacing batteries.

However, the ambient energy is typically sporadic and random, thus making the harvested energy time-varying in addition to the underlying source processes and the channels. Given these variations, the nodes should coordinate their coding and transmission schemes to intelligently manage the energy across the network and achieve the best performance.

Recently, significant research effort has been invested in studying the optimal transmission schemes for EH communication systems [3]–[6]. The classical offline optimization framework deals with systems which assume the non-causal knowledge of the parameters involved, such as energy arrivals, channel gains, etc. See [7] for an overview of different frameworks used in studying EH communication systems.

This work has been performed within the framework of the European research project E-CROPS, funded by CHIST-ERA.

Different from the above mentioned works which deal with throughput optimization, the works [8]–[10] consider the aspects of source sample acquisition, compression rate and transmission with EH constraints in a point-to-point setting. In [9], the problem of distortion minimization in a fading channel with an EH transmitter is considered. Taking into account the variation in energy arrivals, source variances and channel gains, the optimal compression and transmission rates are found using the offline optimization framework. A simple *directional 2D waterfilling* algorithm is proved to be optimal under a strict delay constraint. In [10], the distortion performance is studied using a stochastic EH model.

In this paper, we extend the distortion minimization problem to a network setting. To the best of our knowledge, distributed source coding with EH nodes from a rate-distortion perspective is not studied before. Probably [11] is the closest work that considered distributed compressive sensing in an EH sensor network, however, it ignores transmission and coding aspects. We consider a system of two sensor nodes which observe correlated source samples, and wish to communicate their samples to the destination over orthogonal fading channels with the minimum average end-to-end distortion. The goal is to see how the correlation and the EH affect the coordination among the nodes in compression and transmission schemes. The main contribution of this paper is to characterize the Pareto boundary of the distortion region of the quadratic Gaussian two-encoder source coding problem [12] under EH constraints. As we shall see, the resource allocation policy that optimizes the distortion outperforms the throughput optimization schemes which ignore the variation in source statistics.

II. System model

We consider a system consisting of two sensor nodes where each node observes and samples a common physical phenomenon locally, and hence the samples are correlated. Then the nodes send their information to the destination over orthogonal wireless channels as shown in Fig. 1. Both nodes harvest energy from the environment, and are equipped with individual energy buffers for storage.

A. Energy Harvesting Model

A time slotted system with K unit duration TSs is considered. At the beginning of the k-th TS, $k \in [1:K]$, new energy

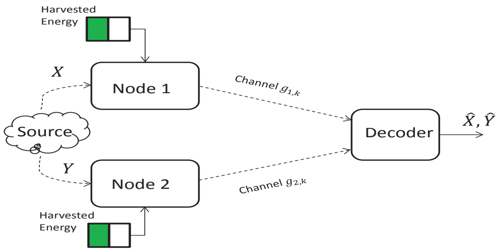

Figure 1. Distributed sensing and transmission with EH nodes.

packets of sizes $e_{1,k}$ and $e_{2,k}$ units arrive at node 1 and 2, respectively. At each node the harvested energy is stored in an infinite size battery and it is used only for communication purposes, i.e., the energy consumed in sampling, compression, etc., is ignored here, and will be studied in a future work.

B. Sensing and Communication Model

The observed physical phenomena at the two nodes are modeled as correlated Gaussian random processes. In the k-th TS, node 1 and node 2 collect samples $\boldsymbol{x}_k^n = [x_{1,k}, x_{2,k}, \ldots, x_{n,k}]$ and $\boldsymbol{y}_k^n = [y_{1,k}\, y_{2,k}, \ldots, y_{n,k}]$, respectively. The elements of $\boldsymbol{x}_k^n$, $\boldsymbol{y}_k^n$ are independent copies of the random variable $\{(X_k, Y_k)\}$, which is modeled as a bi-variate Gaussian random variable with the following probability density function (PDF):

$$f_{X_k,Y_k}(x_k, y_k) = \frac{1}{2\pi|\Lambda_k|^{1/2}} \exp\left\{-\frac{1}{2}\boldsymbol{v}_k{}^T \Lambda_k{}^{-1}\boldsymbol{v}_k\right\},$$

where $\boldsymbol{v}_k = [x_k\ y_k]^{\mathrm{T}}$ and the covariance matrix Λ_k is given by

$$\Lambda_k = \begin{pmatrix} \sigma_{X_k}^2 & \rho_k\sigma_{X_k}\sigma_{Y_k} \\ \rho_k\sigma_{X_k}\sigma_{Y_k} & \sigma_{Y_k}^2 \end{pmatrix},\ -1 < \rho_k < 1.$$

We assume that the duration of each TS is large enough (i.e., large n) to invoke the information theoretic arguments. We consider strict delay constraints, and assume that all samples collected in the beginning of TS k must be sent to the destination within the same TS.

The sensed data is sent to the destination over orthogonal channels. Each TS consists of n channel uses. The channel between the i-th node ($i \in \{1, 2\}$) and the destination in the k-th TS is modeled as a memoryless additive white Gaussian noise (AWGN) channel with unit noise variance and a fixed channel gain $g_{i,k}$. Due to the large n assumption, the maximum transmission rate of the i-th node in the k-th TS is given by $r_{i,k} \triangleq \frac{1}{2}\log_2(1 + g_{i,k}p_{i,k})$ bits/channel use, where $p_{i,k}$ is the average transmission power of node i in k-th TS.

Some comments on the general characteristics of the optimal transmission strategies are in order. First, since the energy packets are available only at the beginning of a TS, and the channel gain remains constant throughout a TS, it is not hard to see that constant power transmission is optimal in each TS, while the transmission power may change from one TS to another. Additionally, since the channels are orthogonal, source-channel separation is optimal in this setting [13].

For a given power/rate allocation, the achievable distortion region in the k-th TS is given by [12]

$$\mathcal{D}_k = \mathcal{D}_{1,k} \cap \mathcal{D}_{2,k} \cap \mathcal{D}_{12,k}, \tag{1}$$

where the sets describing $\mathcal{D}_k$ are defined as:

$$\mathcal{D}_{1,k} = \left\{(d_{1,k}, d_{2,k}) : d_{1,k} \geq \frac{\sigma_{X_k}^2}{2^{2r_{1,k}}}\left(1 - \rho_k^2 + \rho_k^2 2^{-2r_{2,k}}\right)\right\},$$

$$\mathcal{D}_{2,k} = \left\{(d_{1,k}, d_{2,k}) : d_{2,k} \geq \frac{\sigma_{Y_k}^2}{2^{2r_{2,k}}}\left(1 - \rho_k^2 + \rho_k^2 2^{-2r_{1,k}}\right)\right\},$$

and finally,

$$\mathcal{D}_{12,k} = \left\{(d_{1,k}, d_{2,k}) : d_{1,k}d_{2,k} \geq \sigma_{X_k}^2\sigma_{Y_k}^2\beta(r_{1,k}, r_{2,k})\right\},$$

where

$$\beta(r_{1,k}, r_{2,k}) = \rho_k^2 2^{-4(r_{1,k}+r_{2,k})} + \frac{1-\rho_k^2}{2^{2(r_{1,k}+r_{2,k})}},$$

$d_{i,k}$ and $r_{i,k}$ are the achievable distortion and transmission/compression rate of node i in TS k, respectively.

C. Problem Formulation

The distortion achievable for the data transmitted by the i-th sensor node over K TSs is denoted by $D_i = \frac{1}{K}\sum_{k=1}^{K} d_{i,k}$. We define the distortion region $\mathcal{D}^\star$ as

$$\mathcal{D}^\star = \{(D_1, D_2) : (d_{1,k}, d_{2,k}) \in \mathcal{D}_k\ \forall k, (\boldsymbol{p}_1, \boldsymbol{p}_2) \in \mathfrak{F}\},$$

where $\boldsymbol{p}_i = [p_{i,1}, p_{i,2}, \ldots, p_{i,K}], i \in \{1, 2\}$ and $\mathfrak{F}$ is given by

$$\mathfrak{F} = \left\{(\boldsymbol{p}_1, \boldsymbol{p}_2) : \sum_{j=1}^{k} p_{i,j} \leq \sum_{j=1}^{k} e_{i,j},\ p_{i,j} \geq 0, \forall i, \forall k\right\}. \tag{2}$$

The above set represents the *energy neutrality* of the system, i.e., at each node, energy consumed can not be more than the energy harvested till that time.

Our goal is to characterize the *Pareto boundary* of the region $\mathcal{D}^\star$. This boundary consists of operating points (D_1, D_2) such that it is impossible to improve the distortion of one node, without simultaneously increasing the other node's distortion.

III. Characterizing the Pareto Boundary of $\mathcal{D}^\star$

We start by investigating the convexity of $\mathcal{D}^\star$, which will be useful in the characterization of its Pareto boundary. The distortion region in the k-th TS in terms of the transmission powers $p_{i,k}$ can be written as

$$\mathcal{D}_k = \left\{(d_{1,k}, d_{2,k}) : d_{1,k} \geq f_{1,k}, d_{2,k} \geq f_{2,k}, d_{2,k} \geq \frac{f_{12,k}}{d_{1,k}}\right\}, \tag{3}$$

where the functions $f_{1,k} \triangleq f_{1,k}(p_{1,k}, p_{2,k})$, $f_{2,k} \triangleq f_{2,k}(p_{1,k}, p_{2,k})$ and $f_{12,k} \triangleq f_{12,k}(p_{1,k}, p_{2,k})$ are obtained by substituting $r_{i,k} \triangleq \frac{1}{2}\log_2(1 + g_{i,k}p_{i,k})$ in the three sets describing $\mathcal{D}_k$ in (1).

Proposition 1 *The functions* $f_{1,k}(p_{1,k}, p_{2,k})$, $f_{2,k}(p_{1,k}, p_{2,k})$ *and* $\frac{f_{12,k}(p_{1,k},p_{2,k})}{d_{1,k}}$ *are jointly convex in* $p_{1,k}$, $p_{2,k}$ *and* $d_{1,k}$.

Proof: See Appendix. ∎

Proposition 2 *$\mathcal{D}^\star$ is a convex region.*

Proof: Let two distinct distortion pairs achieved by the power allocation policies $(\boldsymbol{p}_1, \boldsymbol{p}_2)$ and $(\tilde{\boldsymbol{p}}_1, \tilde{\boldsymbol{p}}_2)$ belonging to the set $\mathfrak{F}$ be denoted by (D_1, D_2) and $(\tilde{D}_1, \tilde{D}_2)$, respectively. Every point on the line segment joining the points (D_1, D_2) and $(\tilde{D}_1, \tilde{D}_2)$ can be represented by $(\hat{D}_1, \hat{D}_2) = \alpha(D_1, D_2) + (1-\alpha)(\tilde{D}_1, \tilde{D}_2), 0 \leq \alpha \leq 1$. By finding a feasible power allocation policy that achieves the distortion pair $(\hat{D}_1, \hat{D}_2)$, we prove that $\mathcal{D}^\star$ is a convex set. We can write

$$(\hat{D}_1, \hat{D}_2) = \left(\frac{1}{K} \sum_{k=1}^{K} \hat{d}_{1,k}, \frac{1}{K} \sum_{k=1}^{K} \hat{d}_{2,k} \right), \tag{4}$$

where $\hat{d}_{i,k} \triangleq \alpha d_{i,k} + (1-\alpha)\tilde{d}_{i,k},\ i \in \{1,2\}$. Using the conditions in $\mathcal{D}_{1,k}$ we have

$$\begin{aligned} \hat{d}_{1,k} &\geq \alpha f_{1,k}\left(p_{1,k}, p_{2,k}\right) + (1-\alpha) f_{1,k}\left(\tilde{p}_{1,k}, \tilde{p}_{2,k}\right) \\ &\overset{(a)}{\geq} f_{1,k}\left(\hat{p}_{1,k}, \hat{p}_{2,k}\right), \end{aligned} \tag{5}$$

where (a) follows from the convexity of $f_{1,k}$, and the definition $\hat{p}_{i,k} \triangleq \alpha p_{i,k} + (1-\alpha)\tilde{p}_{i,k}$. Similarly, we can show that

$$\hat{d}_{2,k} \geq f_{2,k}\left(\hat{p}_{1,k}, \hat{p}_{2,k}\right). \tag{6}$$

Finally, considering the constraint in $\mathcal{D}_{12,k}$,

$$\begin{aligned} \hat{d}_{2,k} &\geq \alpha \frac{f_{12,k}\left(p_{1,k}, p_{2,k}\right)}{d_{1,k}} + (1-\alpha) \frac{f_{12,k}\left(\tilde{p}_{1,k}, \tilde{p}_{2,k}\right)}{\tilde{d}_{1,k}} \\ &\overset{(b)}{\geq} \frac{f_{12,k}\left(\hat{p}_{1,k}, \hat{p}_{2,k}\right)}{\hat{d}_{1,k}}, \end{aligned} \tag{7}$$

where (b) follows from the convexity of $f_{12,k}/d_{1,k}$.

Since $(\boldsymbol{p}_1, \boldsymbol{p}_2) \in \mathfrak{F}$ and $(\tilde{\boldsymbol{p}}_1, \tilde{\boldsymbol{p}}_2) \in \mathfrak{F}$, it can be easily seen that $(\hat{\boldsymbol{p}}_1, \hat{\boldsymbol{p}}_2) \in \mathfrak{F}$. From (5), (6) and (7), we have $(\hat{d}_{1,k}, \hat{d}_{2,k}) \in \mathcal{D}_k$. Using (4) and the definition of $\mathcal{D}^\star$, we conclude that $(\hat{D}_1, \hat{D}_2) \in \mathcal{D}^\star$, and hence the proof. ∎

Since $\mathcal{D}^\star$ is a convex region, the Pareto boundary is the closure of all the points $(\mathrm{D}_1^\star, \mathrm{D}_2^\star)$, where $(\mathrm{D}_1^\star, \mathrm{D}_2^\star)$ is the solution to the following optimization problem

$$\min_{(D_1, D_2)} \mu_1 D_1 + \mu_2 D_2 \quad \text{s.t } (D_1, D_2) \in \mathcal{D}^\star \tag{8}$$

for some $\boldsymbol{\mu} = [\mu_1\ \mu_2]^{\mathrm{T}} \in \mathbb{R}_+^2$. We examine two different cases of (8) depending on the choice of $\boldsymbol{\mu}$.

A. Source coding with a helper node ($\mu_1 = 0$ or $\mu_2 = 0$)

In this subsection, we focus on the scenario in which the decoder is interested in minimizing the distortion of one of the source component, and treats the other component information as side information. Without loss of generality, we consider minimizing the distortion D_1. Since the decoder is only interested in decoding X_k, the distortion incurred in decoding Y_k, $d_{2,k}$, is ignored. Thus, in this case the distortion region is given by [14]

$$\mathcal{D}_k = \Big\{ (d_{1,k}, d_{2,k}) : d_{1,k} \geq f_{1,k}(p_{1,k}, p_{2,k}) \Big\}. \tag{9}$$

The power allocation policy that minimizes D_1 is obtained by solving the following optimization problem

$$\min_{p_{i,k}, d_{1,k}} \quad \sum_{k=1}^{K} d_{1,k} \tag{10a}$$

$$f_{1,k}(p_{1,k}, p_{2,k}) - d_{1,k} \leq 0, \quad k \in [1:K] \tag{10b}$$

$$\sum_{j=1}^{l} p_{i,j} \leq \sum_{j=1}^{l} e_{i,j},\ i \in \{1,2\},\ l \in [1:K], \tag{10c}$$

$$p_{i,k} \geq 0 \quad i \in \{1,2\},\ k \in [1:K]. \tag{10d}$$

Since the distortion is minimized, the constraint (10b) is satisfied with equality for the optimal solution. Using Proposition 1, we can see that (10) is a convex optimization problem, and the Karush-Kuhn-Tucker (KKT) conditions provide the necessary and sufficient conditions for optimality [15]. The Lagrangian of (10) can be defined as

$$\begin{aligned} \mathcal{L} \triangleq &\sum_{k=1}^{K} f_{1,k}(p_{1,k}, p_{2,k}) + \sum_{j=1}^{K} \lambda_j \left(\sum_{k=1}^{j} p_{1,k} - \sum_{k=1}^{j} e_{1,k} \right) \\ &+ \sum_{j=1}^{K} \psi_j \left(\sum_{k=1}^{j} p_{2,k} - \sum_{k=1}^{j} e_{2,k} \right) + \sum_{k=1}^{K} \eta_k p_{1,k} + \sum_{k=1}^{K} \phi_k p_{2,k}, \end{aligned} \tag{11}$$

where $\lambda_j \geq 0, \psi_j \geq 0, \eta_k \geq 0$ and $\phi_k \geq 0$ are the Lagrange multipliers corresponding to (10c) and (10d). Taking the derivative of (11) with respect to $p_{1,k}$, and using the complimentary slackness conditions, we obtain

$$p_{1,k} = W_k \left[\vartheta_k - H_k \right]^+, \tag{12}$$

where $W_k \triangleq \sqrt{\frac{\sigma_{X_k}^2}{g_{1,k}} \left(1 - \rho_k^2 + \frac{\rho_k^2}{(1+p_{2,k} g_{2,k})} \right)}$, $H_k \triangleq \frac{1}{W_k g_{1,k}}$ and the water level $\vartheta_k \triangleq \frac{1}{\left(\sqrt{\sum_{j=k}^{K} \lambda_j} \right)}$. Similarly,

$$p_{2,k} = B_k \left[\gamma_k - L_k \right]^+, \tag{13}$$

where $B_k \triangleq \frac{\sigma_{Y_k} \rho_k}{\sqrt{g_{2,k}(1+p_{1,k} g_{1,k})}}$, $L_k \triangleq \frac{1}{B_k g_{2,k}}$ and the water level $\gamma_k \triangleq \frac{1}{\sqrt{\sum_{j=k}^{K} \psi_j}}$, From (12) and (13) we can see that optimal $p_{i,k}$'s are dependent, and it is difficult to obtain a closed form expression, however, an iterative directional 2D waterfilling algorithm to obtain the optimal policy is provided.

Given the optimal power allocation of the second node, denoted as $\boldsymbol{p}_2^*$, the optimal $\boldsymbol{p}_1^*$ is obtained by solving

$$\min_{p_{1,k}} \sum_{k=1}^{K} f_{1,k}(p_{1,k}, p_{2,k}^*) \text{ s.t } (\boldsymbol{p}_1, \boldsymbol{p}_2^*) \in \mathfrak{F}. \tag{14}$$

By using KKT conditions, it can be easily seen that $p_{1,k}^*$ is obtained by plugging $p_{2,k}^*$ into the expression in (12). This solution can be interpreted as directional 2D water-filling [9]. A graphical illustration of the solution for $p_{1,k}^*$ is given in Fig. 2, for $K=3$ TSs. Precisely, in the k-th TS we have rectangles of width W_k and height H_k. The harvested energy is poured over the level H_k up to the water level ϑ_k. The shaded area below the water level ϑ_k and above H_k represents the power

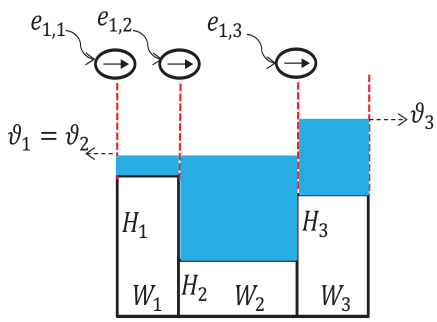

Figure 2. 2D waterfilling interpretation.

allocated in TS k. The directional taps in Fig. 2 represents the fact that the energy can be flown only in forward direction. We refer the reader to [9] for the details of the algorithm.

Since (10) is a convex optimization problem, and the constraint set can be written as the Cartesian product of two sets, it can be shown that an alternating minimization algorithm, alternating between vectors $\boldsymbol{p}_1$ and $\boldsymbol{p}_2$, converges to the global optimum [16]. Therefore, we use directional 2D water-filling in an alternating fashion until the solution converges. We denote $(\mathrm{D}_{1,m}, \mathrm{D}_{2,h})$ as the optimal distortion tuple obtained when $\mu_2 = 0$. Similarly, we obtain $(\mathrm{D}_{1,h}, \mathrm{D}_{2,m})$ when $\mu_1 = 0$.

B. *Weighted sum distortion* ($\mu_1 > 0, \mu_2 > 0$)

The points in between $(\mathrm{D}_{1,m}, \mathrm{D}_{2,h})$ and $(\mathrm{D}_{1,h}, \mathrm{D}_{2,m})$ that lie on the Pareto boundary are obtained by solving (8) for $\boldsymbol{\mu} > 0$. The optimization problem is given by

$$\min_{p_{i,k}, d_{i,k}} \quad D_s = \mu_1 \sum_{k=1}^{K} d_{1,k} + \mu_2 \sum_{k=1}^{K} d_{2,k} \tag{15a}$$

$$(d_{1,k}, d_{2,k}) \in \mathcal{D}_k, \;\; k \in [1:K] \tag{15b}$$

$$(\boldsymbol{p}_1, \boldsymbol{p}_2) \in \mathfrak{F}. \tag{15c}$$

Since $\mathcal{D}_k$ is a convex set (by Proposition 2), and the other constraints are linear, (15) is a convex optimization problem. To further understand the structure of the optimal solution, the optimization is performed in two steps. First, consider

$$\tilde{D}_s\left(\boldsymbol{p}_1, \boldsymbol{p}_2\right) = \min_{d_{i,k}} D_s \text{ s.t } (d_{1,k}, d_{2,k}) \in \mathcal{D}_k \; \forall k. \tag{16}$$

We now illustrate the solution of (16) graphically in Fig. 3. Since there is no dependency among the distortion sets $\mathcal{D}_i, \mathcal{D}_j, i \neq j$, the optimization can be performed separately for each TS. In the k-th TS, depending on the slope of the line $\mu_1 d_{1,k} + \mu_2 d_{2,k}$, it is not hard to see that the optimal solution must occur at one the following three points:

$$(d^*_{1,k}, d^*_{2,k}) = \begin{cases} \mathrm{A} \triangleq \left(f_{1,k}, \dfrac{f_{12,k}}{f_{1,k}}\right), \\ \mathrm{B} \triangleq \left(\dfrac{f_{12,k}}{f_{2,k}}, f_{2,k}\right), \text{ or} \\ \mathrm{C} \triangleq \left(\sqrt{\dfrac{\mu_2}{\mu_1}} f_{12,k}, \sqrt{\dfrac{\mu_1}{\mu_2}} f_{12,k}\right), \end{cases} \tag{17}$$

as shown in Fig. 3. Since (15) is a convex optimization problem, the function $\tilde{D}_s$ is convex with domain $\{(\boldsymbol{p}_1, \boldsymbol{p}_2) : (\boldsymbol{p}_1, \boldsymbol{p}_2) \in \mathfrak{F}, (d_{1,k}, d_{2,k}) \in \mathcal{D}_k \forall k\}$ [15, 3.2.5].

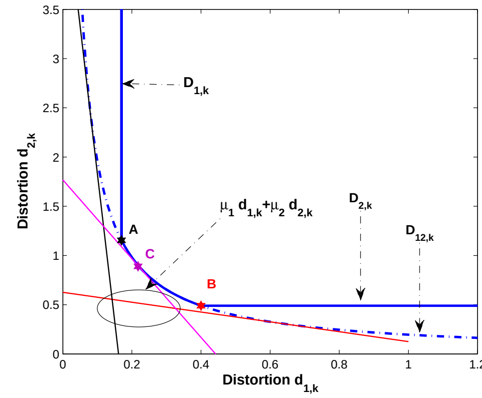

Figure 3. Distortion region $\mathcal{D}_k$, lines $\mu_1 d_{1,k} + \mu_2 d_{2,k}$ for different $\boldsymbol{\mu}$.

Using (16) and (17), the second step of the optimization is given by

$$\min_{p_{i,k}} \quad \tilde{D}_s\left(\boldsymbol{p}_1, \boldsymbol{p}_2\right) = \mu_1 \sum_{k=1}^{K} d^*_{1,k} + \mu_2 \sum_{k=1}^{K} d^*_{2,k} \tag{18a}$$

$$(\boldsymbol{p}_1, \boldsymbol{p}_2) \in \mathfrak{F}. \tag{18b}$$

Using the above analysis, we now provide a simplified way of obtaining the Pareto optimal points of $\mathcal{D}^*$ in a static setting.

1) Static setting: In the static setting, we have $\sigma^2_{X_k} = \sigma^2_X, \sigma^2_{Y_k} = \sigma^2_Y, \rho_k = \rho, g_{i,k} = g_i, \forall i, k$, and the EH profiles are *similar*. The EH profiles are said to be similar if the most majorized[1] feasible vectors $(\boldsymbol{p}^*_1, \boldsymbol{p}^*_2)$, where $\boldsymbol{p}^*_1 \preceq \boldsymbol{p}_1, \boldsymbol{p}^*_2 \preceq \boldsymbol{p}_2, \forall (\boldsymbol{p}_1, \boldsymbol{p}_2) \in \mathfrak{F}$, have same structure i.e., $\forall k$, if $p^*_{1,k} = p^*_{1,k+1}$ then $p^*_{2,k} = p^*_{2,k+1}$, and if $p^*_{1,k} \neq p^*_{1,k+1}$ then $p^*_{2,k} \neq p^*_{2,k+1}$. More details can be found in [17, Sec. V-A].

Proposition 3 *In the static setting, all points on the Pareto boundary of $\mathcal{D}^*$are obtained by the power allocation $(\boldsymbol{p}^*_1, \boldsymbol{p}^*_2)$, where $\boldsymbol{p}^*_1 \preceq \boldsymbol{p}_1, \boldsymbol{p}^*_2 \preceq \boldsymbol{p}_2 \; \forall (\boldsymbol{p}_1, \boldsymbol{p}_2) \in \mathfrak{F}$.*

Proof: In the static case, we have $f_{i,k}(p_{1,k}, p_{2,k}) = f_i(p_{1,k}, p_{2,k}) \forall i, k$ and $f_{12,k}(p_{1,k}, p_{2,k}) = f_{12}(p_{1,k}, p_{2,k}) \forall k$. Therefore, using (17) in the static setting, we can write $d^*_{i,k}(p_{1,k}, p_{2,k}) = d^*_i(p_{1,k}, p_{2,k}) \forall i, k$. Since $d^*_{i,k} = d^*_i \forall k$, we can see that the function $\tilde{D}_s\left(\boldsymbol{p}_1, \boldsymbol{p}_2\right)$ is symmetric. Using the convexity and symmetry of $\tilde{D}_s$, and by [17, Proposition 4], we can prove that $(\boldsymbol{p}^*_1, \boldsymbol{p}^*_2)$ is optimal. Once $(\boldsymbol{p}^*_1, \boldsymbol{p}^*_2)$ is obtained, the optimal distortion region $\mathcal{D}^*_k$ for TS k is given by (1). Depending on $\boldsymbol{\mu}$, using $\mathcal{D}^*_k$ and (17), we obtain $(d^*_{1,k}, d^*_{2,k})$ and then $(\mathrm{D}^\star_1, \mathrm{D}^\star_2)$. ■

We could not find a simple algorithm to solve (15) in a non-static setting, therefore we resort to numerical methods.

IV. Numerical Results

In this section, numerical simulations are used to illustrate the Pareto boundary of the distortion region. We consider $K = 6$ TSs. The harvested energy vectors are chosen as

[1] $\boldsymbol{x} \preceq \boldsymbol{y}$ denotes that the vector $\boldsymbol{x}$ is *majorized* by the vector $\boldsymbol{y}$. Please refer to [17] for details.

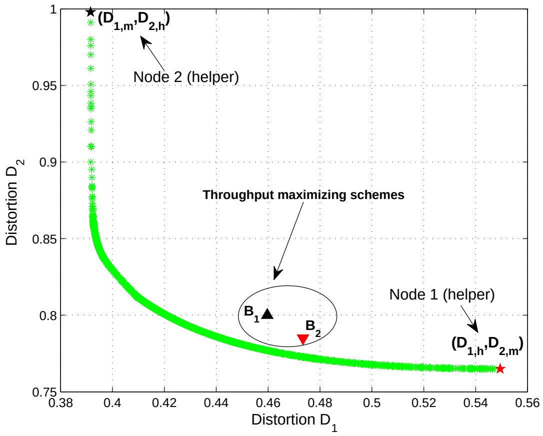

Figure 4. Pareto boundary of $\mathcal{D}^*$.

$\boldsymbol{e}_1 = [4, 2, 5, 4, 3, 10]$ and $\boldsymbol{e}_2 = [4, 0.5, 3.5, 2.5, 3, 4]$. The variance of the sources are given by $\boldsymbol{\sigma}_X^2 = [3, 0.2, 2, 0.4, 1.4, 0.3]$ and $\boldsymbol{\sigma}_Y^2 = [0.8, 2, 3.6, 4.8, 1.2, 2.3]$. The correlation coefficient among the observed source samples is $\boldsymbol{\rho} = [0.95, 0.4, 0.5, 0.3, 0.8, 0.1]$. Fig. 3 shows the Pareto boundary of $\mathcal{D}^\star$ when the channel gains are chosen as $\boldsymbol{g}_1 = [0, 0.9, 0.2, 0, 0.8, 0.3]$ and $\boldsymbol{g}_2 = [0.5, 0, 0.8, 0.9, 0.1, 0.9]$. The points $(\mathrm{D}_{1,m}, \mathrm{D}_{2,h})$ and $(\mathrm{D}_{1,h}, \mathrm{D}_{2,m})$ correspond to the distortion pairs when node 2 or node 1 acts as the helper node, respectively. The remaining boundary, shown in green in Fig. 4, is obtained by numerically solving (15) for different $\boldsymbol{\mu} \in \mathbb{R}_+^2$ pairs. The points B_1 and B_2 are obtained when each node greedily maximizes the total number of bits transmitted till the end of K-th TS irrespective of the source statistics. In each TS, at each node, the compression rate is equal to the transmission rate. The power allocation at i-th node is obtained by using directional waterfilling with $\boldsymbol{e}_i$ and $\boldsymbol{g}_i$ [4].

V. Conclusion

We have determined the Pareto boundary of the the distortion region of the quadratic Gaussian two-encoder source coding problem with EH nodes. Specific points on this boundary are obtained by using an iterative directional 2D waterfilling algorithm. In the static case, we have shown that all points on the Pareto boundary are obtained by the most majorized feasible power allocation policies.

Appendix

A. Proof of Proposition 1

Since $r_{i,k}$ is concave in $p_{i,k}$, it can be easily seen that $2^{-r_{1,k}}$ and $2^{-(r_{1,k}+r_{2,k})}$ are convex. Since the summation of convex functions is convex, $f_1(p_{1,k}, p_{2,k})$ is convex. Similarly, we can show that $f_2(p_{1,k}, p_{2,k})$ is also convex. To show that the final function is convex as well, consider the following functions:

$$h(x) = \sqrt{\rho_k^2 2^{-4x} + (1-\rho_k^2) 2^{-2x}},$$

and $g(x, d_{1,k}) = \frac{x^2}{d_{1,k}}$. The derivative of h is given by

$$h^{'}(x) = -\log_e 2 \left[h(x) + \frac{\rho_k^2}{\sqrt{\rho_k^2 16^x + (1-\rho_k^2) 64^x}} \right].$$

It can be seen that $h^{'}(x)$ is monotonically increasing, and therefore $h(x)$ is convex. The function $g(x, d_{1,k})$ is convex for $d_{1,k} > 0$ [15]. Using the above defined functions we can write

$$\frac{f_{12}(p_{1,k}, p_{2,k})}{d_{1,k}} = g\left(h\left(p_{1,k}, p_{2,k}\right), d_{1,k}\right), \tag{19}$$

where $h(p_{1,k}, p_{2,k}) = h(r_{1,k} + r_{2,k})$.

The function $h(p_{1,k}, p_{2,k})$ is convex since $h(x)$ is convex and non-increasing, and $r_{i,k}$ is concave. Using the fact that $h(p_{1,k}, p_{2,k})$ and $g(x, d_{1,k})$ are convex, and monotonicity of g in the first argument, we can easily prove that $\frac{f_{12}(p_{1,k}, p_{2,k})}{d_{1,k}}$ is convex.

References

[1] A. Kansal, J. Hsu, S. Zahedi, and M. B. Srivastava, "Power management in energy harvesting sensor networks," *ACM Trans. Embed. Comput. Syst.*, vol. 6, no. 4, Sep. 2007.

[2] S. Sudevalayam and P. Kulkarni, "Energy harvesting sensor nodes: survey and implications," *IEEE Communications Surveys Tutorials*, vol. 13, no. 3, pp. 443–461, Mar. 2011.

[3] J. Yang and S. Ulukus, "Optimal packet scheduling in an energy harvesting communication system," *IEEE Trans on Comm.*, vol. 60, no. 1, pp. 220–230, Jan. 2012.

[4] O. Ozel, K. Tutuncuoglu, J. Yang, S. Ulukus, and A. Yener, "Transmission with energy harvesting nodes in fading wireless channels: optimal policies," *IEEE JSAC*, vol. 29, no. 8, pp. 1732–1743, Sep. 2011.

[5] C. K. Ho and R. Zhang, "Optimal energy allocation for wireless communications with energy harvesting constraints," *IEEE Transactions on Signal Processing*, vol. 60, no. 9, pp. 4808–4818, Sep. 2012.

[6] O. Orhan, D. Gunduz, and E. Erkip, "Energy harvesting broadband communication systems with processing energy cost," *IEEE Transactions on Wireless Communications*, vol. 13, no. 11, pp. 6095–6107, Nov. 2014.

[7] D. Gunduz, K. Stamatiou, N. Michelusi, and M. Zorzi, "Designing intelligent energy harvesting communication systems," *IEEE Communications Magazine*, vol. 52, no. 1, pp. 210–216, Jan. 2014.

[8] P. Castiglione, O. Simeone, E. Erkip, and T. Zemen, "Energy management policies for energy-neutral source-channel coding," *IEEE Trans on Communications*, vol. 60, no. 9, pp. 2668–2678, Sep. 2012.

[9] O. Orhan, D. Gunduz, and E. Erkip, "Source-channel coding under energy, delay and buffer constraints," 2014. [Online]. Available: http://arxiv.org/abs/1501.01858

[10] M. Motlagh, M. Khuzani, and P. Mitran, "On lossy source-channel transmission in energy harvesting communication systems," in *IEEE ISIT*, June 2014.

[11] W. Chen, Y. Andreopoulos, I. Wassell, and M. Rodrigues, "Towards energy neutrality in energy harvesting wireless sensor networks: A case for distributed compressive sensing?" in *IEEE GLOBECOM*, Dec 2013.

[12] A. Wagner, S. Tavildar, and P. Viswanath, "Rate region of the quadratic Gaussian two-encoder source-coding problem," *IEEE Transactions on Information Theory*, vol. 54, no. 5, pp. 1938–1961, May. 2008.

[13] J.-J. Xiao and Z.-Q. Luo, "Multiterminal source-channel communication over an orthogonal Multiple-access channel," *IEEE Transactions on Information Theory*, vol. 53, no. 9, pp. 3255–3264, Sep. 2007.

[14] Y. Oohama, "Gaussian multiterminal source coding," *IEEE Trans on Info Theory*, vol. 43, no. 6, pp. 1912–1923, Nov. 1997.

[15] S. Boyd and L. Vandenberghe, *Convex optimization*. New York, NY, USA: Cambridge University Press, 2004.

[16] D. Bertsekas, *Nonlinear programming*. Athena Scientific, 1999.

[17] R. Gangula, D. Gesbert, and D. Gunduz, "Optimization of energy harvesting MISO communication system with feedback," *IEEE JSAC*, vol. 33, no. 3, pp. 396–406, Mar 2015.